Quantum Kinetic Theory of Phonon-Assisted Excitation Transfer in Quantum Dot Molecules

Emil Rozbicki* and Paweł Machnikowski†

Institute of Physics, Wrocław University of Technology, 50-370 Wrocław, Poland

(Received 22 August 2007; published 16 January 2008)

We present a quantum-kinetic theory of the excitation transfer in a quantum dot molecule. We derive the consistent Markovian limit for the system kinetics, which leads to a description in terms of a single transfer rate for weak coupling. We show that the transfer rate is a strongly varying, nonmonotonic function of the spatial separation and energy mismatch between the dots.

DOI: 10.1103/PhysRevLett.100.027401 PACS numbers: 78.67.Hc, 03.65.Yz, 71.38.−k, 73.63.Kv

Current manufacturing technologies allow one to produce semiconductor structures built of nearly identical quantum dots (QDs), with the splitting of the ground state transition energies down to a few meV [1,2]. Since the QDs forming such structures are electronically coupled [3,4], they are referred to as quantum dot molecules (QDMs). For QDMs with separations of several nm, carrier tunneling is exponentially suppressed [5] and the energetically lowest states correspond to spatially direct excitons [6]. Such states are bound by the Coulomb interaction via static [7–9] and interband [9,10] dipole moments. The latter is referred to as the Förster interaction, and its signatures were found, e.g., in a photon-correlation experiment [1].

While the static (''direct'') dipole coupling preserves the occupations of the individual QDs, the Förster interaction provides for a transfer of occupation between the dots. In the presence of a dissipation channel, this excitation transfer may become irreversible. For confined carriers, the dissipation is dominated by phonon-related mechanisms. In spite of the importance of the excitation transfer for current experiments [1,5,11–14], relatively little theoretical effort has been devoted to the role of phonons in this process [15–18] and the existing theory is mostly restricted to perturbative (Fermi golden rule) approaches [16,18] or Förster phenomenology [15]. No attempt has been made to describe the system dynamics in the general case, when the excitation of one of the QDs does not necessarily correspond to an eigenstate of the unperturbed system and, therefore, the Fermi golden rule is of no use.

In this Letter we propose a rigorous quantum-kinetic description of the phonon-assisted Förster transfer of an exciton in a QDM. As we will show, the general evolution of the system involves an interplay of coherent dynamics and relaxation. The main result of the Letter is the consistent Markovian approximation to the system kinetics, which is particularly useful in the limit of weak coupling. The resulting transfer rate is a nonmonotonic, oscillating function of the QD energy mismatch and spatial separation and cannot be correctly reproduced by the Förster phenomenological approach [19]. Nonetheless, it can still be estimated using experimentally measurable characteristics of the QDM. Finally, we show that the transfer may be much faster than suggested by the existing perturbative estimates [16].

We consider two flat, cylindrically symmetric, coaxial QDs, separated by the distance D along the z axis [see inset in Fig. 1(c)] and interacting with phonons. The formalism will be restricted to the subspace spanned by the states $|1\rangle$, $|2\rangle$, corresponding to a single exciton in the ground state of the ''dot 1'' and ''dot 2,'' respectively (with a fixed polarization). We assume that the wave functions of excitons confined in different dots do not overlap, which excludes phonon-assisted tunneling. The Hamiltonian of the system is then $H = H_0 + H_I$, where

$$H_0 = \frac{1}{2}\Delta\sigma_z + V\sigma_x + \hbar\sum_{\boldsymbol{k}}\omega_{\boldsymbol{k}} b_{\boldsymbol{k}}^\dagger b_{\boldsymbol{k}} \tag{1}$$

and the carrier-phonon interaction Hamiltonian is

$$H_I = \sum_{l=1,2}|l\rangle\langle l|\sum_{\boldsymbol{k}}(g_{\boldsymbol{k}}^{(l)} b_{\boldsymbol{k}} + g_{\boldsymbol{k}}^{(l)*} b_{\boldsymbol{k}}^\dagger). \tag{2}$$

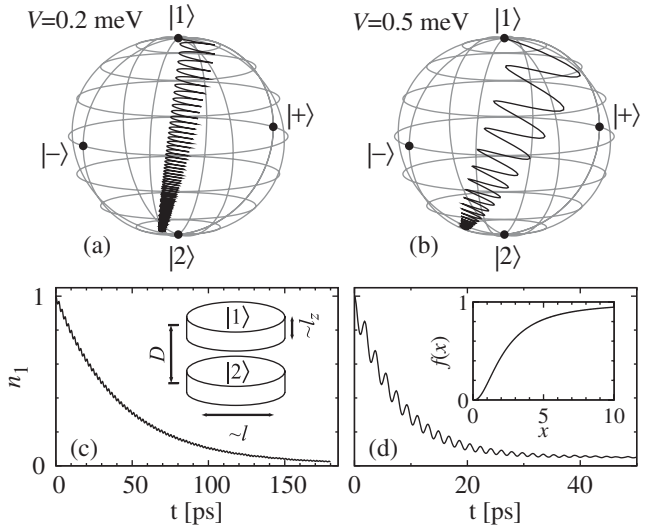

FIG. 1. (a),(b) The Bloch sphere representation of the evolution for two coupling strengths. (c),(d) The corresponding occupation of the ''dot 1'' as a function of time. The results are calculated at $T = 4$ K. Inset in (c): the system geometry. Inset in (d): the correction to the dipole approximation.

Here σ_i are Pauli matrices in the basis of the states $|1\rangle$, $|2\rangle$, $\Delta > 0$ is the energy mismatch between the dots, V is the amplitude of the Förster coupling, $b_{\boldsymbol{k}}^{\dagger}$, $b_{\boldsymbol{k}}$ are creation and annihilation operators for the phonon mode with a wave vector $\boldsymbol{k}$, $\omega_{\boldsymbol{k}}$ is the corresponding frequency, and $g_{\boldsymbol{k}}^{(i)}$ are exciton-phonon coupling constants.

We assume Gaussian wave functions for electrons and holes (identical in both dots) of the form $\psi_{e,h}(\boldsymbol{r}) \sim \exp\{-[(x^2 + y^2)/l_{e,h}^2 + z^2/l_z^2]/2\}$. In the calculations we will use $l_e = 4.4$ nm, $l_h = 4.0$ nm, and $l_z = 1$ nm.

For heavy-hole excitons confined in QDs stacked along z one has

$$V = \frac{e^2|a|^2}{4\pi\epsilon_0\epsilon_r D^3}\frac{l^2}{l_e l_h} f(D/l),$$

where e is the electron charge, ϵ_0 and ϵ_r are the vacuum and relative dielectric constants, $l^2 = (1/l_e^2 + 1/l_h^2)^{-1}$, and $a = \hbar P_{\mathrm{cv}}/(m_0 E_g) \approx \hbar/\sqrt{2m_e E_g}$ [20], where P_{cv} is the interband matrix element of the momentum operator, m_0 and m_e are the free and effective electron masses, and E_g is the band gap. The function $f(x)$ accounts for the correction to the dipole approximation [16] and can be represented as

$$f(x) = \frac{x^3}{\sqrt{2\pi}}\int_0^1 dt(1-t^2)\frac{u(t) - x^2t^2}{u^{5/2}(t)}\exp\left[-\frac{x^2t^2}{2u(t)}\right],$$

where $u(t) = 1 - t^2 + \lambda^2 t^2$ and $\lambda = l_z/l$ [see inset in Fig. 1(d)]. We focus on a self-assembled InAs/GaAs system; hence, $|a|$ should lie between the GaAs and InAs values of 0.6 nm and 1.88 nm, respectively [21]. An estimate based on the exciton radiative lifetime of 500 ps [1] yields $|a_{\mathrm{QD}}| = 0.86$ nm. One should note that, in contrast to the Förster interaction, the static dipole coupling is diagonal in the occupation eigenstates and its only effect is to shift the energy of the biexciton state. Therefore its presence or absence does not affect the dynamics in the restricted, single-exciton subspace and is therefore irrelevant to the present study.

The most effective interaction between neutral excitons and phonons is the deformation potential coupling to longitudinal acoustic modes [22]. For Gaussian wave functions one gets [23] $g_{\boldsymbol{k}}^{(0,1)} = g_{\boldsymbol{k}} e^{\pm ik_z D/2}$, with

$$g_{\boldsymbol{k}} = (\sigma_e - \sigma_h)\sqrt{\frac{\hbar k}{2\rho v c}}e^{-l^2(k_x^2+k_y^2)/4 - l_z^2 k_z^2/4},$$

where σ_e, σ_h are the deformation potential constants for electrons and holes, ρ is the crystal density, c is the speed of sound, and v is the normalization volume. We take $\sigma_e - \sigma_h = 9$ eV, $\rho = 5350$ kg/m^3, $c = 5150$ m/s, and $\epsilon_r = 10.9$.

The common way of describing the evolution of an interacting carrier-phonon system in a QD is the correlation expansion (CE) technique [24–26]. We have numerically solved the relevant evolution equations up to the two-phonon-assisted level [26] in the frequency representation [27] on a nonuniform grid of 700 points with a higher density around the resonant frequency and with a frequency cutoff at 20 ps^{-1}. Thus, we treat the problem at a sufficient level to account for the coherent and nonequilibrium phonons, which are important for the carrier-phonon kinetics in QDs [26]. We assume that initially a single exciton is localized in the "dot 1."

The evolution of the exciton subsystem in a QDM with $D = 6$ nm and $\Delta = 2$ meV at $T = 4$ K is represented in the Bloch sphere picture in Figs. 1(a) and 1(b). The two values of the Förster coupling $V = 0.2$ meV and $V = 0.5$ meV correspond to $|a| = 1$ nm and $|a| = 1.6$ nm, respectively. As can be seen in the plots, the system evolution is a combination of a rotation around a tilted axis, defined by the eigenstates of H_0, and damping resulting from the interaction with phonons. As a result of the latter, at low temperatures the system relaxes towards the lower eigenstate of H_0 (with a small correction due to polaron effects). This evolution is reflected by the decaying occupation of the initial state [Figs. 1(c) and 1(d)], which has the form of oscillations around an exponential curve.

For $V \ll \Delta$, the lower eigenstate is close to the state $|2\rangle$ and the transfer to the lower-energy dot is practically indistinguishable from exponential, as can be seen in Fig. 2. Here and henceforth we fix $|a| = |a_{\mathrm{QD}}| = 0.86$ nm. From the results of the quantum-kinetic calculations presented in Fig. 2, it is clear that the charge transfer rate is a nonmonotonic, oscillating function of both the energy mismatch [Fig. 2(a)] and the QD separation [Fig. 2(b)].

In the following, we will derive a simple but highly accurate description accounting for this behavior. To this end, we write the time-convolutionless (TCL) evolution equation [28] for the exciton density matrix in the interaction picture with respect to H_0 [Eq. (1)],

$$\dot{\rho}(t) = -\int_0^t d\tau_{\mathrm{ph}}[H_I(t), [H_I(\tau), \rho(t) \otimes \rho_{\mathrm{ph}}]], \quad (3)$$

where $H_I(t)$ is the interaction Hamiltonian [Eq. (2)] in the interaction picture and ρ_{ph} is the phonon density matrix at the thermal equilibrium. The evolution is conveniently

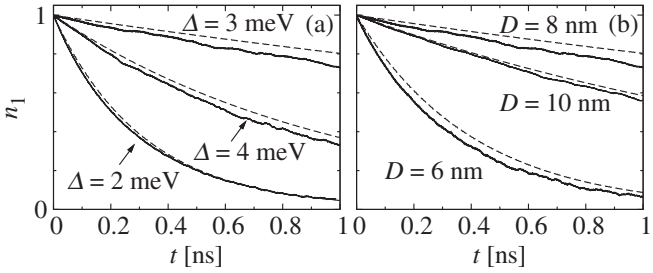

FIG. 2. The occupation of the higher energy QD as a function of time at $T = 4$ K: (a) $D = 8$ nm and Δ as shown; (b) $\Delta = 3$ meV and D as shown. Dashed line: the Markov approximation with renormalized coupling.

described by writing the state as $\rho(t) = (1/2)[1 + \boldsymbol{r}(t) \cdot \tilde{\boldsymbol{\sigma}}]$, where $\tilde{\boldsymbol{\sigma}}$ is the vector of Pauli matrices written in the eigenbasis of H_0 (thus $\boldsymbol{r}$ is the Bloch vector in the interaction picture). Then Eq. (3) leads to

$$\dot{\boldsymbol{r}}(t) = \boldsymbol{s}(t) \times [\boldsymbol{u}(t) \times \boldsymbol{r}(t) - \boldsymbol{v}(t)], \tag{4}$$

where $\boldsymbol{s}(t) = (-\sin 2\phi \cos 2\Delta t, \sin 2\phi \sin 2\Delta t, \cos 2\phi)$, $\phi = (1/2)\arcsin(2V/\sqrt{\Delta^2 + 4V^2})$,

$$\boldsymbol{u}(t) = \int_0^t d\tau \boldsymbol{s}(\tau)\mathcal{R}(t-\tau) + \text{H.c.}, \tag{5a}$$

$$\boldsymbol{v}(t) = i\int_0^t d\tau \boldsymbol{s}(\tau)\mathcal{R}(t-\tau) + \text{H.c.}, \tag{5b}$$

and $\mathcal{R}(t)$ is the memory function defined as

$$\mathcal{R}(t) = \frac{2}{\hbar^2}\sum_{\boldsymbol{k}} \sin^2\frac{k_z D}{2}|g_{\boldsymbol{k}}|^2[(n_{\boldsymbol{k}}+1)e^{-i\omega_{\boldsymbol{k}}t} + n_{\boldsymbol{k}}e^{i\omega_{\boldsymbol{k}}t}],$$

where $n_{\boldsymbol{k}}$ are phonon occupation numbers. In Fig. 3(a) we show the initial stage of the decay for $\Delta = 2$ meV, $D = 6$ nm, and $V = 0.13$ meV ($a = a_{\text{QD}}$), comparing the result from the TCL equations (dashed line) to that obtained by the CE calculations (solid line). The results are close to each other, although the TCL method yields a slightly faster decay.

The next step towards a convenient description of excitation transfer is to consistently approximate the non-Markovian quantum-kinetic description by Markovian equations. We represent the memory function as

$$\mathcal{R}(t) = \int_{-\infty}^{\infty} d\omega R(\omega) e^{-i\omega t}, \tag{6}$$

where the spectral density of the phonon reservoir

$$R(\omega) = \frac{2}{\hbar^2}|n_B(\omega)+1|\sum_{\boldsymbol{k}}\sin^2\frac{k_z D}{2}|g_{\boldsymbol{k}}|^2\delta(|\omega| - \omega_{\boldsymbol{k}})$$

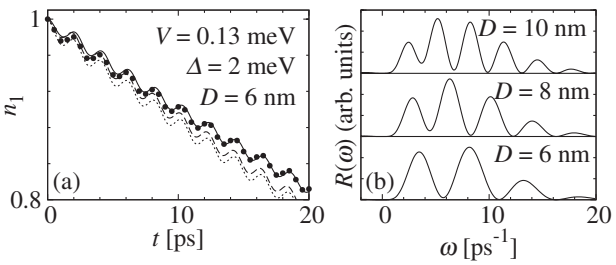

FIG. 3. (a) The initial stage of the transfer from "dot 1" at $T = 4$ K, obtained in different approximations: CE (solid line), TCL (dashed line), Markov-RWA (dotted line), and Markov-RWA with renormalized coupling (thick points). (b) The phonon spectral density of the QDM at $T = 4$ K.

vanishes at $\omega \to 0$ and for $\omega \gg c/l_z$ [Fig. 3(b)]. Here $n_B(\omega)$ is the Bose distribution. Inserting Eq. (6) into Eq. (5a) we find for the first component of $\boldsymbol{u}(t)$

$$u_1(t) = -2\sin 2\phi \int_{-\infty}^{\infty} d\omega R(\omega)\left[\frac{\sin\frac{\omega+\Omega}{2}t\cos\frac{\omega-\Omega}{2}t}{\omega+\Omega} + \frac{\sin\frac{\omega-\Omega}{2}t\cos\frac{\omega+\Omega}{2}t}{\omega-\Omega}\right],$$

where $\Omega = \sqrt{\Delta^2 + 4V^2}/\hbar$ is the resonant frequency corresponding to the splitting between the eigenstates of H_0. In the long time limit, using the identity $\sin(xt)/x \to \pi\delta(x)$ and repeating the procedure for all the components of $\boldsymbol{u}(t)$ and $\boldsymbol{v}(t)$ one finds $u_{1,2}(t) = \pi s_{1,2}(t)\gamma$, $u_3(t) = 0$, $v_{1,2}(t) = \mp\pi s_{2,1}(t)\beta$, and $v_3(t) = -2s_3\int_{-\infty}^{\infty} d\omega R(\omega)/\omega$, where $\gamma = [R(\Omega) + R(-\Omega)]$ and $\beta = [R(\Omega) - R(-\Omega)]$.

Finally, we make the rotating wave approximation (RWA), which, in the present formalism, corresponds to discarding all the oscillating terms appearing in Eq. (4) in the Markovian approximation (that is, $\cos\Omega t \to 0$, $\cos^2\Omega t \to 1/2$, etc.). As a result, one gets

$$\dot{r}_{1,2} = -\frac{\pi}{2}\gamma\sin^2 2\phi r_{1,2}, \qquad \dot{r}_3 = -\pi\sin^2 2\phi(\gamma r_3 + \beta),$$

which means that the system relaxation follows the universal optical Bloch equations with the rate $\Gamma = \pi\sin^2 2\phi\gamma$, determined by the phonon spectral density of the QDM (note, however, that $\boldsymbol{r}$ represents the system state in the interaction picture and in the basis of eigenstates of H_0). The system evolution obtained in this approximation is plotted in Fig. 3(a) (dotted lines). Comparison to the results of the non-Markovian TCL equations shows that the Markovian approximation introduces only a minor inaccuracy. In fact, the discrepancy between the CE results and the TCL and Markov approximations is mostly due to the phonon-induced renormalization of the coupling [25]. To the leading order, the latter consists in reducing the coupling V to $\tilde{V} = V[1 - \int_{-\infty}^{\infty} d\omega R(\omega)/\omega^2]$. With this correction, the Markovian approximation yields reasonably accurate results, as shown in Fig. 2 (dashed line) and Fig. 3 (points).

The rate for the phonon-assisted process is governed, on the one hand, by the amplitude of the Förster coupling, which decreases roughly as $1/D^3$. On the other hand, it is strongly influenced by the structure of $R(\omega)$. In particular, it has a pronounced minimum whenever Δ is a multiple of $2\pi\hbar c/D$, which explains the oscillating dependence on both Δ and D (see Fig. 4). These oscillations lead to a strong dependence on the system parameters. For instance, for $D = 6$ nm [Fig. 4(a)] the rate drops by 2 orders of magnitude when the energy mismatch Δ increases from 1.8 meV to 3.8 meV and then grows again by an order of magnitude as Δ further increases by 1 meV. Similar,

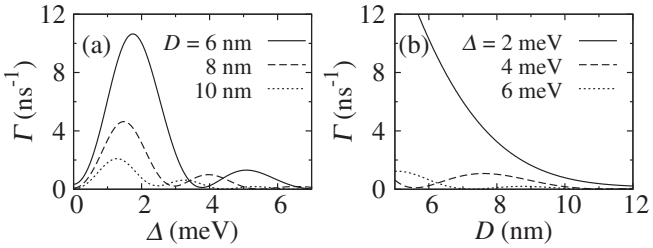

FIG. 4. The rate of phonon-assisted excitation transfer as a function of the energy mismatch for a few values of the QD separation D (a) and as a function of D for a few values of Δ (b) at $T = 4$ K.

although less pronounced, oscillations appear in the dependence on the separation D [Fig. 4(b)].

In general, upon transforming back to the original basis $|1\rangle$, $|2\rangle$ and to the Schrödinger picture one obtains a complex evolution as in Figs. 1(a) and 1(b). However, in the case of $|V| \ll |\Delta|$, which is of particular practical importance, one finds $\sin 2\phi \approx 2V/|\Delta|$. Moreover, in this limit the eigenstates of H_0 are very close to $|1\rangle$ and $|2\rangle$. In this way one obtains an exponential excitation transfer with the rate $\Gamma \approx 4\pi(\tilde{V}/\Delta)^2\gamma$. Let us note that this rate cannot be reproduced within the original Förster phenomenology [19] based on the spectral overlap of the absorption and emission spectra, even if the phonon sidebands are included in the line shapes. Indeed, the oscillating features are absent from the phonon side bands of a single dot [22], as well as of a QDM. The latter follows from the explicit evolution of the elements of the density matrix related to the optical polarization for a QDM [29], where no dependence on the distance D appears. Still, in the weak coupling limit and for the geometry discussed here, a "rule of thumb" for estimating the transfer rate from experimentally measurable spectral features can be extracted from the theory, since the envelope of $(1/2)R(\omega)/\omega^2$ corresponds to the phonon sideband in the normalized spectrum of the QD optical response [22]. This must be taken at $\omega = \pm\Delta$ and multiplied by $4\pi V^2$ and by the QDM interference factor $2\sin^2[\omega D/(2c)]$.

In conclusion, we have presented a theory of the phonon-assisted excitation transfer between quantum dots. We started from the full quantum-kinetic description and derived a consistent Markovian approximation, which becomes particularly simple in the weak coupling limit. The obtained transfer rates show very strong, nonmonotonic dependence on the system parameters. We have also pointed out that the transfer rate can be deduced from the optical spectra of the QDs and from the QDM geometry.

This work was supported by the Polish MNiSW (No. N202 1336 33). P. M. is grateful to V. M. Axt for inspiring discussions on the correlation expansion.

*Present address: School of Physics and Astronomy, University of St. Andrews, St. Andrews, Fife, U.K.
†Pawel.Machnikowski@pwr.wroc.pl

[1] B. D. Gerardot *et al.*, Phys. Rev. Lett. **95**, 137403 (2005).
[2] G. Ortner *et al.*, Phys. Rev. B **71**, 125335 (2005).
[3] M. Bayer *et al.*, Science **291**, 451 (2001).
[4] H. J. Krenner *et al.*, Phys. Rev. Lett. **94**, 057402 (2005).
[5] T. Nakaoka *et al.*, Phys. Rev. B **74**, 121305(R) (2006).
[6] B. Szafran, S. Bednarek, and J. Adamowski, Phys. Rev. B **64**, 125301 (2001).
[7] E. Biolatti, R. C. Iotti, P. Zanardi, and F. Rossi, Phys. Rev. Lett. **85**, 5647 (2000).
[8] T. Unold *et al.*, Phys. Rev. Lett. **94**, 137404 (2005).
[9] J. Danckwerts, K. J. Ahn, J. Forstner, and A. Knorr, Phys. Rev. B **73**, 165318 (2006).
[10] B. W. Lovett, J. H. Reina, A. Nazir, and G. A. D. Briggs, Phys. Rev. B **68**, 205319 (2003).
[11] R. Heitz, I. Mukhametzhanov, P. Chen, and A. Madhukar, Phys. Rev. B **58**, R10151 (1998).
[12] A. Tackeuchi *et al.*, Phys. Rev. B **62**, 1568 (2000).
[13] S. Rodt *et al.*, Phys. Rev. B **67**, 235327 (2003).
[14] G. Ortner *et al.*, Phys. Rev. B **72**, 165353 (2005).
[15] A. O. Govorov, Phys. Rev. B **68**, 075315 (2003).
[16] A. O. Govorov, Phys. Rev. B **71**, 155323 (2005).
[17] M. Richter *et al.*, Phys. Status Solidi (b) **243**, 2302 (2006).
[18] A. Thilagam and M. A. Lohe, arXiv:cond-mat/0702428.
[19] T. Förster, Discuss. Faraday Soc. **27**, 7 (1959).
[20] P. Y. Yu and M. Cardona, *Fundamentals of Semiconductors* (Springer, Berlin, 2005), 3rd ed.
[21] S. Adachi, *Handbook on Physical Properties of Semiconductors* (Kluwer, Boston, 2004), Vol. 2.
[22] B. Krummheuer, V. M. Axt, and T. Kuhn, Phys. Rev. B **65**, 195313 (2002).
[23] A. Grodecka and P. Machnikowski, Phys. Rev. B **73**, 125306 (2006).
[24] J. Förstner, C. Weber, J. Danckwerts, and A. Knorr, Phys. Rev. Lett. **91**, 127401 (2003).
[25] A. Krügel *et al.*, Appl. Phys. B **81**, 897 (2005).
[26] A. Krügel, V. M. Axt, and T. Kuhn, Phys. Rev. B **73**, 035302 (2006).
[27] E. Rozbicki and P. Machnikowski, Acta Phys. Pol. A **112**, 197 (2007).
[28] H.-P. Breuer and F. Petruccione, *The Theory of Open Quantum Systems* (Oxford University Press, Oxford, 2002).
[29] K. Roszak and P. Machnikowski, Phys. Rev. A **73**, 022313 (2006).